A high-resolution gridded dataset of daily temperature and precipitation records (1980 – 2018) for Trentino – South Tyrol (north-eastern Italian Alps)

Alice Crespi[1], Michael Matiu[1], Giacomo Bertoldi[2], Marcello Petitta[1,3], Marc Zebisch[1]

5 [1]Institute for Earth Observation, Eurac Research, Bolzano, 39100, Italy
[2]Institute for Alpine Environment, Eurac Research, Bolzano, 39100, Italy
[3]SSPT-MET-CLIM, ENEA, Rome, 00196, Italy

Correspondence to: Alice Crespi (alice.crespi@eurac.edu)

Abstract. A high-resolution gridded dataset of daily mean temperature and precipitation series spanning the period 1980 –
10 2018 was built for Trentino – South Tyrol, a mountainous region in north-eastern Italy, starting from an archive of observation
series from more than 200 meteorological stations, covering the regional domain and surrounding countries. The original
station data underwent a processing chain including quality and consistency checks, homogeneity tests, with the
homogenization of the most relevant breaks in the series, and a filling procedure of daily gaps aiming at maximizing the data
availability. Using the processed database, an anomaly-based interpolation scheme was applied to project the daily station
15 observations of mean temperature and precipitation onto a regular grid of 250 m x 250 m resolution. The accuracy of the
resulting dataset was evaluated by the leave-one-out station cross-validation. Averaged over all sites, interpolated daily
temperature and precipitation show no bias, with a mean absolute error (MAE) of about 1.5 °C and 1.1 mm and a mean
correlation of 0.97 and 0.91, respectively. The obtained daily fields were used to discuss the spatial representation of selected
past events and the distribution of the main climatological features over the region, which shows the role of the mountainous
20 terrain in defining the temperature and precipitation gradients. In addition, the suitability of the dataset to be combined with
other high-resolution products was evaluated through a comparison of the gridded observations with snow-cover maps from
remote sensing observations. The presented dataset provides an accurate insight on the spatio-temporal distribution of
temperature and precipitation over the mountainous terrain of Trentino – South Tyrol and a valuable support for local and
regional   applications.   The   dataset   is   publicly   available   at
25 https://www.pangaea.de/tok/2bea918566a8c18a728e098858856cd1fcc8dbe4, Crespi et al. (2020).

1 Introduction

High-resolution gridded datasets of in situ climate observations are of increasing relevance not only for the studies on climate
and its variability but also for many applications, such as natural resource management, adaptation planning, modelling and
risk assessment in a wide range of fields including hydrology, agriculture and energy (Haylock et al., 2008; Hofstra et al.,

30   2008). For instance, spatialized in situ observations can be used in runoff, crop growth and glacier mass balance modelling (Engelhardt et al., 2014; Ledesma and Futter, 2017), to validate and bias-correct climate simulations (Kotlarski et al., 2019; Navarro-Racines et al., 2020), to calibrate and integrate remote sensing products (Schlögel et al., 2020) and to develop advanced monitoring systems supporting decision making (Aadhar and Mishra, 2017). This is particularly meaningful for local studies over topographically complex areas experiencing a high climatic heterogeneity, such as the Alps, where the Italian

35   region of Trentino – South Tyrol is located. Mountain areas are essential for freshwater and hydropower production, and they are particularly prone to natural hazards such as floods, landslides and avalanches which threat human life and infrastructures and require monitoring and prevention (Immerzeel et al., 2020).

Several gridded products of temperature and precipitation series are currently available globally, at European and at national scales at different spatial resolutions, for example WorldClim at ~ 5 km horizontal spacing (Harris et al., 2014; Fick and

40   Hijmans, 2017), E-OBS for Europe at ~ 10 km resolution (Haylock et al. 2008), GAR-HRT (Chimani et al., 2013), APGD and LAPrec (Isotta et al., 2014; Isotta et al., 2019) for Alps at around 5 km grid spacing. The datasets are derived by applying interpolation methods to the meteorological station records unevenly located over the territory to obtain estimates for each point of a regular grid. The accuracy of the results depends on the available station coverage, which could be particularly sparse for some mountain areas. However, the spatial resolution of the large-scale gridded products (from few to tens of km)

45   does not allow to properly capture the finer climate gradients of mountainous regions such as Trentino – South Tyrol and to respond to the needs of local applications. Further gridded data were computed at transregional, sub-regional and catchment levels at different timescales and at finer resolution, generally 1 km horizontal spacing (e.g. Brunetti et al., 2012; Laiti et al. 2018), however most of them cover only partially the study region and/or are not up to date, which limits their applicability for operational purposes.

50   The choice of the horizontal resolution of the gridded products is handled differently by the different communities. From a climatological point of view, developing kilometre scale or even sub-kilometre scale products based on interpolated sparse observations does not provide more information than deriving coarser products (Haylock et al., 2008). The effective resolution is mostly defined by the underlying station distribution and it can be different from the target grid spacing (Grasso, 2000; Lussana et al., 2019). However, from a user perspective, higher resolution data might be more desirable, because they are

55   closer to the actual problems for practical applications (Beven et al., 2015), requiring a precise definition of local gradients which in mountainous terrains can occur over distances less than 1 km. Even if they contain similar information as their coarser resolution counterparts, a sensible interpolation approach of climate variables to finer spatial scales is beneficial, especially in highly complex mountain terrains such as Trentino – South Tyrol, to properly account for the orographic gradients in a wide range of applications, e.g. modelling of snow, hydrological processes, vegetation or heat-related health impacts. Moreover,

60   high-resolution data can be used more conveniently in hydrological models or for processing satellite observations without the need of a further downscaling.

Different interpolation techniques have been developed so far to derive gridded climate products and the choice largely depends on the domain features, data availability and desired spatial details. The proposed methods include inverse distance weighting

(IDW, Camera et al., 2014), splines (Stewart and Nitschke, 2017), geostatistical schemes such as kriging and its variants
65 (Hengl, 2009; Sekulić et al., 2020), optimal interpolation (Lussana et al., 2019) and regression-based approaches (Daly et al.,
2007; Brunsdon et al., 2001). In topographically complex domains the interpolation schemes modelling the relationship
between the terrain features and the climate gradients are preferable (Daly et al., 2002). However, the spatialization methods
are required to deal with the heterogeneity of observation availability, which typically decreases e.g. in high-elevation
mountain regions, where only over recent decades new automatic meteorological stations have been settled and provide
70 information for previously uncovered areas.

Geostatistical and regression-based methods computing local gradients require dense data coverages and could provide
unreliable spatial patterns where data density is low and strong spatial variability occurs, especially for precipitation fields and
at daily timescale (Hofstra et al., 2010; Ly et al., 2011; Crespi et al., 2018). More straightforward approaches, such as IDW,
could provide more stable results even though the final spatial variability could result highly smoothed and affected by
75 over/underestimations if data are unevenly distributed (Di Piazza et al., 2011). In order to partially overcome these issues,
anomaly-based methods were proposed in which the final gridded daily distribution for a certain variable is obtained by
superimposing the long-term climatological values of reference, generally 30 year means, and the spatial distribution of the
local daily deviations from them (e.g. New et al., 2001). Especially for daily precipitation, the interpolation with a reference
field and anomalies was proved to be less prone to errors than the direct interpolation of absolute values, such as systematic
80 underestimations in high-mountain regions due to the prevalence of stations located in the low valleys (Isotta et al., 2014;
Crespi et al., 2021). This concept was applied in a relevant number of studies (see e.g. Haylock et al., 2008; Brunetti et al.,
2012; Chimani et al., 2013; Hiebl and Frei, 2018; Longman et al., 2019).

In this work, we present the gridded dataset of daily mean temperature and precipitation for Trentino – South Tyrol region
covering a 39 year period (1980 – 2018) at very high spatial resolution (250 m). The gridded dataset is computed from a
85 collection of more than 200 daily station records retrieved from the regional meteorological network and checked for quality
and homogeneity. The daily interpolation is based on the anomaly concept by superimposing the 1981 – 2010 daily
climatologies at 250 m resolution computed by a weighted linear regression with topographic features and the 250 m resolution
fields of daily anomalies obtained by a weighted-averaging approach. To the authors' knowledge, this is the first time such
interpolation scheme is applied to derive daily fields of these two key climatic variables at such a fine grid spacing. The
90 resulting gridded climate product includes the small-scale terrain features of the region and can be easily integrated and
combined with models and other high-resolution data, e.g. remote sensing observations, without applying any further
downscaling to get a target sub-kilometre scale. In addition, the resulting product was designed to be regularly updated by the
recent station records in order to respond to more operational purposes.

Section 2 describes the collection and processing of the meteorological station data and provides a detailed explanation of the
95 applied interpolation technique. In Sect. 3 the accuracy of the gridded dataset is discussed on the basis of the results of cross-
validation analyses, and the regional climate features and selected examples derived from the computed fields are presented.
In addition, a preliminary comparison of the 250 m gridded temperature and precipitation series with the 2001 – 2018 winter

snow cover data from remote sensing images over the region is reported in order to provide further insights into the potential applications of the dataset and its suitability in being combined with other high-resolution products. Section 4 provides the
100 information about the dataset availability and access. Finally, the summary of the main outcomes and outlooks of the work are reported in Sect. 5.

2 Data and Methods

2.1 The study area

Trentino – South Tyrol is a region located in north-eastern Italy covering an area of around 13,000 km^2 (Fig. 1). Its territory is
105 entirely mountainous, including a large portion of Dolomites and southern Alps and it is located at the intersection region for various types of air masses: humid influences from the Atlantic northwest, dry air masses from the continental east, typically experiencing cold winters and warm summers, and warm contributions from the Mediterranean area bringing humid winters and dry summers (Adler et al., 2015). The geographical location and the complex topography of the region determine a strong climate variability and contribute to define small-scale effects in the spatial distribution of temperature and precipitation (Price,
110 2009). The territory is characterized by strong altitude gradients with very narrow valleys surrounded by steep slopes. Elevation range extends from 65 m a.s.l. in the areas close to Lake Garda in the south to 3905 m a.s.l. of the Ortler peak in the Stelvio National Park (north-west). The mean elevation of the region is around 1600 m with only 4% of flat areas, i.e. with slope steepness below 5%. The main valley is the one of Adige River, the second longest Italian river, flowing from Reschen Pass in the north-western corner of the region to the Adriatic Sea. Adige River flows through Venosta Valley with a west-to-east
115 orientation and then it crosses the entire region north-to-south. Its main tributary is Isarco River which defines the second major valley of South Tyrol flowing from the Brenner Pass (north of Vipiteno) to Bolzano city.
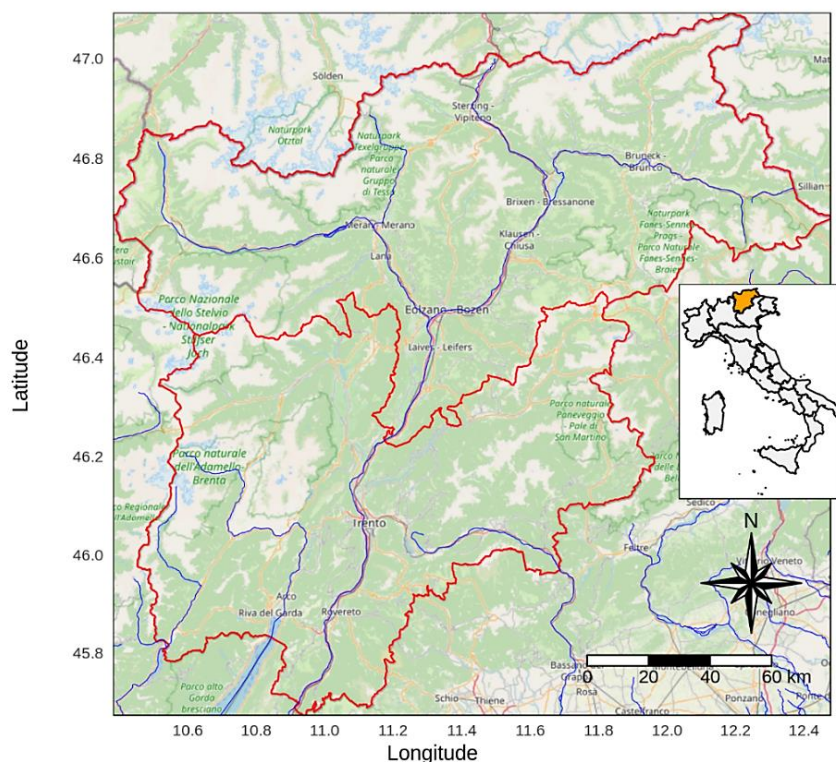
Figure 1: The study region of Trentino – South Tyrol composed by the Autonomous Provinces of Trento and Bolzano (red bordered) and the region location in Italy (orange area in the inset plot). [© OpenStreetMap contributors 2020. Distributed under a Creative Commons BY-SA License]

2.2 The observation database

The database used for the present study was set up by retrieving the observation series of daily maximum and minimum temperature (T_{max}, T_{min}) and daily total precipitation (P) from the stations of the meteorological networks of Trentino – South Tyrol region. More precisely, the data for the Autonomous Province of Trento were received from Meteotrentino (https://www.meteotrentino.it/), while the meteorological series for the Autonomous Province of Bolzano were provided by the Hydrographic Office. In total 311 series of daily T_{max} and T_{min} and 243 series of daily P were collected (Fig. 2). The series were integrated with the records from few close sites located in surrounding regions, especially in the north where the terrain is mainly mountainous, and the less dense regional coverage could not be enough to provide a suitable representation of climate gradients in the high-Alpine environment over the borders. At this aim, some daily series from Switzerland, Austria and Veneto were also included. Swiss sites were retrieved from MeteoSwiss (IDAWEB, https://gate.meteoswiss.ch/idaweb/), Veneto data were provided by the Regional Agency of Environmental Protection (ARPA Veneto), while Austrian series were provided by the Zentralanstalt für Meteorologie und Geodynamik (ZAMG). In addition, data for some further Austrian locations were

collected from the HISTALP database of daily homogenized records (Auer et al., 2007;
130   http://www.zamg.ac.at/histalp/dataset/station/csvHOMSTART.php).

From around the 1990s, the manual measurements were replaced by automatic stations in most meteorological services. In this study we did not distinguish between manual and automatic records and their consistency was assured by quality-check and homogenization procedures (see below for details on quality-check and homogeneity tests). In addition, the observation time and meteorological day definition slightly vary among the networks and could change within the years, especially in the shift
135   from manual to automatic systems. For instance, daily precipitation records from the regional network are generally referred to the cumulated precipitation from 08:00 UTC of previous day to the 08:00 UTC of current day and also the recent automatic records are defined by following this definition. However, this information is not always reported, and other daily reading times could have been adopted in some cases such as 07:00 UTC and 00:00 UTC. Clear shifts due to changes in time coding were checked and corrected, but no specific correction of the observation time was applied and induced inhomogeneities were
140   assessed through the quality-check procedures.

The collected database spanned the period from 1950 to present and the whole interval was used for the quality-check and homogenization procedures in order to increase the statistics and the robustness of the analyses. The series in close proximity (horizontal distance < 3 km and vertical distance < 100 m) but covering different time periods were merged in order to improve the length and continuity of available records. The merging concerned mostly some stations for Trentino province, which were
145   split due to slight relocations and/or after the transition from mechanical to automatic sensors.

Quality-check analyses were performed on the daily series of T_{max}, T_{min} and P in order to detect outliers and to assess the spatial and temporal consistency of data. Implausible values, such as negative precipitation and out-of-range records, were scanned by setting fixed thresholds. In particular, P exceeding 500 mm, T_{min} < -40 °C, T_{min} > +40 °C, T_{max} < -30 °C, T_{max} > +50 °C and diurnal temperature range > 35 °C were considered and removed if not supported by metadata or by surrounding station
150   records. In addition, cases of daily T_{min} exceeding T_{max} were invalidated and periods of continuous null daily P over more than one month were detected and removed if a simultaneous dry period was not reported for nearby sites. Temporal consistency was also scanned in both T_{max} and T_{min} series by searching for differences in consecutive days greater than 20 °C (Durre et al., 2010).

In order to further assess the general quality of the series, monthly records were computed and each one was simulated over
155   the whole spanned period by means of the surrounding station data (Crespi et al., 2018). The comparison between monthly observed and simulated values allowed to detect stations affected by frequent malfunctions and further periods of suspicious records. After these quality controls, 11 temperature series and 13 precipitation series with low-quality data or duplicates of other series were discarded from the following analyses.

After the quality-check, all series with more than 30 years of valid records underwent homogeneity controls and the ones
160   showing relevant breaks were homogenized. To this aim, the Craddock test (Craddock, 1979) was applied to the monthly records by using as reference the 5 nearby stations with the highest number of data in common. In some cases, the comparison with the available homogenized records from HISTALP and MeteoSwiss supported the identification of possible breaks. The

daily homogenization of records with relevant breaks was then performed by computing the monthly correcting factors and by extracting from them through a trigonometric fitting the daily adjustments to be applied to each calendar day over the inhomogeneous period. If T_{max} and T_{min} series were corrected, their internal consistency was checked to be preserved. In total 48 P series, 11 T_{max} series and 13 T_{min} series were homogenized. Short periods with strong breaks for which no robust correction factors could be computed were invalidated. We adopted a precautionary approach and no correction was performed if the non-climatic nature of the deviation could not be identified clearly.

As last step, in order to increase the data coverage and to maximize the temporal extent of the records, a gap-filling procedure was applied to reconstruct the missing daily data. The filling was performed by considering the data of the surrounding station with the highest correlation with the data of series under evaluation and by rescaling its daily value for the ratio (in case of precipitation) and the difference (in case of temperature) of the daily averages of the two series over a common subset of data, which is defined by a window centred on the daily gap and extending over both years and days. The reconstruction was performed only if the test series contained at least 70% of valid daily data in the selected window and a total of around 8000 daily entries was reconstructed over the period 1980 – 2018.

All processed series with less than 10 years of records were discarded from the database used for the interpolation since they could not provide robust long-term references from which the anomalies were computed. Daily mean temperature series were finally derived as the average of T_{max} and T_{min} values.

The resulting database contained 236 daily mean temperature and 219 daily precipitation series, 205 and 188 out of them located within the region, respectively (Fig. 2). The best data coverage is between 500 and 1500 m for both temperature and precipitation databases, while the number of available stations is almost halved for higher elevation bands (Fig. 3). The database did not include precipitation sites above 3000 m.
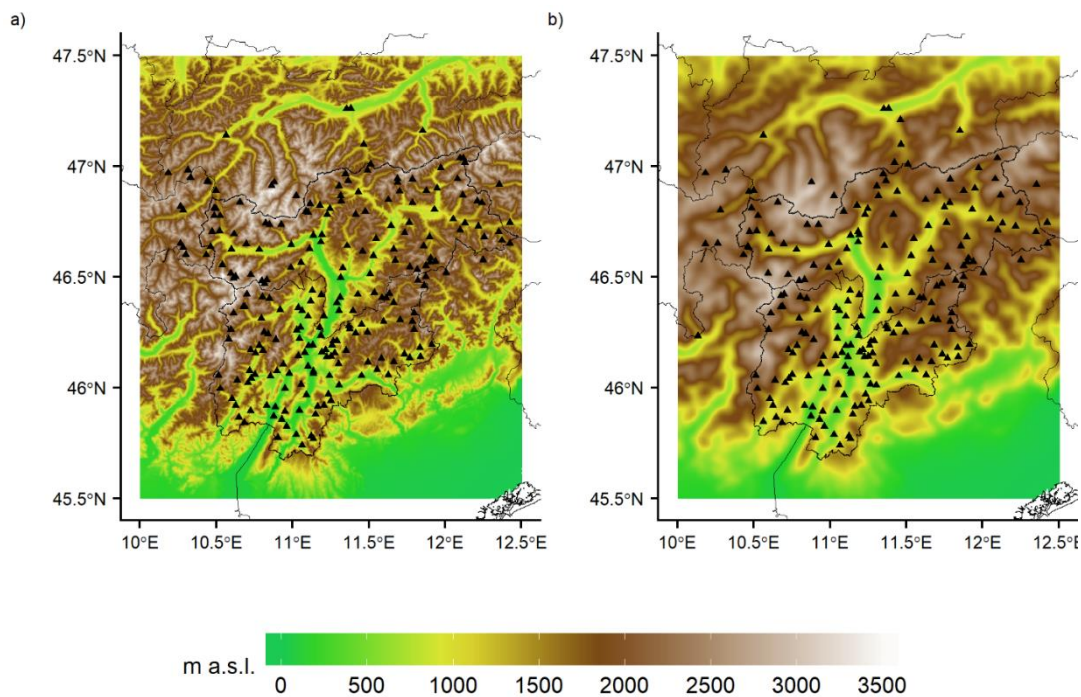
Figure 2: Spatial distribution of a) temperature and b) precipitation weather stations superimposed to the topography considered in the interpolation scheme. In panel a) the DEM at 250 m resolution is reported, in panel b) the smoothed version of the 250 m DEM used for precipitation spatialization is shown.
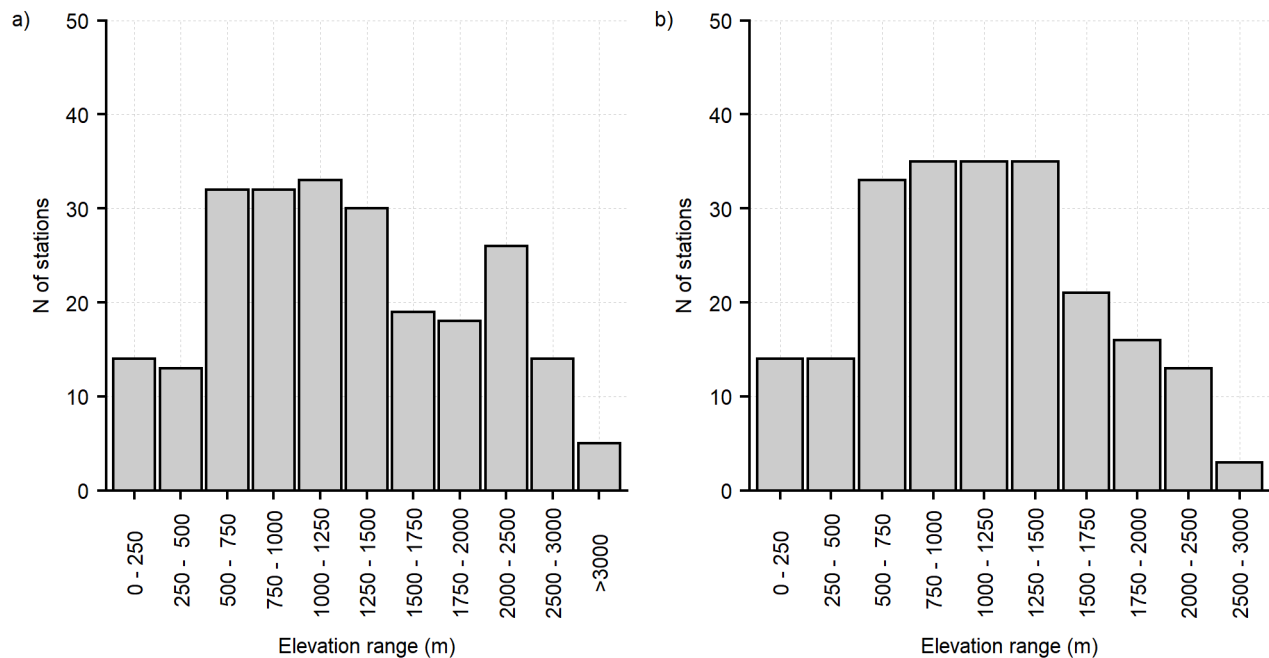
Figure 3: Available a) temperature and b) precipitation stations over different elevation ranges.

However, the data availability is not constant over time (Fig. 4). The first relevant improvement of data coverage occurs during the 1970s, while the greatest increase is observed after 1980 and, especially for temperature, after 1990 when the automatic

185 stations started to operate in most areas. Due to the significantly lower station availability before the 1980s, which could reduce the general accuracy of the results for the early decades, the starting year for the computation of the gridded dataset for both temperature and precipitation was set to 1980. Although the coverage of temperature series is less dense than that of precipitation data before 1990, this it is not expected to affect the general robustness of the results thanks to the greater spatial coherence typically shown by temperature records (Brunetti et al., 2006). The effects of the variability in data availability on

190 the result accuracy was discussed more in detail in Sect. 3.1.
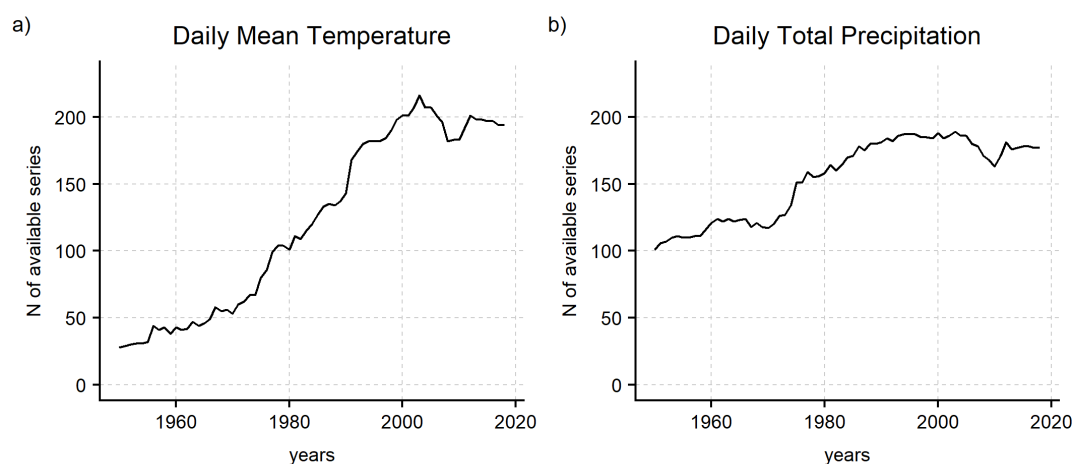
Figure 4: Number of available stations over 1950 – 2018 period in the collected databases of a) temperature and b) precipitation.

2.3 The interpolation scheme

The 250 m resolution fields of daily mean temperature and daily precipitation over Trentino – South Tyrol were computed over the period 1980 – 2018 by applying the anomaly-based approach. In this framework, the final gridded output is derived

195 from the superimposition of the gridded station daily anomalies and the interpolated climatologies, i.e. 30 year means, for the reference period 1981 – 2010. The interpolation grid and all topographic features were derived from the Digital Elevation Model (DEM) Copernicus EU-DEM v1.1 (https://land.copernicus.eu/imagery-in-situ/eu-dem/eu-dem-v1.1), which was aggregated from the original 25 m to the target 250 m resolution. The elevation values of the DEM used for precipitation interpolation were further smoothed by replacing the elevation of each point by a weighted average of the surrounding grid

200 cell elevations with weights halving at 2 km distance from the considered cell. The halving distance was chosen as the one minimizing the modelling errors (see Sect. 3.1 for a description of errors). This procedure was introduced in order to avoid including in the interpolation too detailed terrain gradients with respect to the actual spatial scales of interaction between atmospheric circulation and orography (Brunetti et al., 2012; Foresti et al., 2018). In the following the two steps of the interpolation procedure are described, separately.

2.3.1 The 1981 – 2010 climatologies

In order to derive the 1981 – 2010 climatological fields of mean temperature and precipitation, the daily series were aggregated at monthly scale and the monthly climatological normals, defined as the averages over the 30 year period, were computed for each station in the database. In order to prevent the station normals from being biased due to the different number of available monthly data over 1981 – 2010, before their calculation, all missing monthly values in the reference interval for each series were reconstructed by means of the nearby stations (Brunetti et al., 2014; Crespi et al., 2018).

The monthly station normals were interpolated at each point of the 250 m resolution grid based on the PRISM scheme developed by Daly et al. (2002) and applying a weighted linear regression with elevation where weights vary locally and depend on geographical features. In particular, the climatology z for the month m at the target grid point (x, y) is derived as:

$$z_m(x, y) = a_m(x, y) + b_m(x, y) \cdot h(x, y) \tag{1}$$

where $a_m(x, y)$ and $b_m(x, y)$ are the regression coefficients for the point (x, y) and month m and $h(x, y)$ is the point elevation. The regression coefficients were derived for each grid cell by a weighted linear fit with the 35, for temperature, and 15, for precipitation, surrounding stations with the highest weights. The station weight depends on the distance and orographic similarities, in terms of elevation, slope steepness and orientation, with the grid point under evaluation. The weight contribution of station i at the target point (x, y) for each geographic parameter par was defined on a monthly basis by a Gaussian function:

$$w_{i,m}^{par}(x, y) = e^{-\left(\frac{\left(\Delta_{i,m}^{par}(x,y)\right)^2}{c_m^{par}}\right)} \tag{2}$$

where $\Delta_{i,m}^{par}$ is the difference in the geographical parameter between the station i and the grid point, and c is the decay coefficient which was kept constant over the domain and optimized for each month by means of an iterative procedure. The total station weight was derived as product of the single weighting functions of geographical parameters. The number of stations entering in the fit was also defined by the same optimization procedure minimizing the model errors.

2.3.2 The daily anomalies and the absolute fields

The fields of daily mean temperature and daily precipitation anomalies were computed over the period 1980 – 2018 for the 250 m resolution grid. To this aim, the station daily records were converted into series of daily anomalies. More precisely, for mean temperature, the daily normals of each station were firstly obtained by interpolating the corresponding monthly normals by means of the first two harmonics of a Fourier series and the daily anomalies were then computed as the difference between the daily observed temperature and the daily normal for the corresponding calendar day. As regards precipitation, daily anomalies were defined as the direct ratio between the daily precipitation record and the climatological value of the corresponding month.

The station daily anomalies were interpolated onto the grid through a weighted averaging approach considering horizontal and vertical distances between the station and the grid cell. In the case of precipitation, in order to reduce the simulation of false

235   wet days, the interpolated precipitation was set to zero if no precipitation was recorded at the three closest stations on the day under reconstruction.

Finally, the gridded anomalies were combined with the 1981 – 2010 climatologies to derive the daily fields of mean temperature and precipitation in absolute values. As regards temperature, for each point of the grid the daily climatological references were obtained by fitting the modelled monthly climatologies by means of the same trigonometric fit used at station

240   level and they were added to the corresponding interpolated daily anomalies. The absolute fields for precipitation were obtained by multiplying the gridded anomalies and the monthly normals of the corresponding calendar month.

All data processing and interpolation routines were implemented and run by the authors under R environment (https://www.r-project.org/).

3 Results and Discussion

245   **3.1 The dataset validation**

The uncertainty evaluation of the gridded datasets is essential to properly apply the products and interpret the results. One of the most important aspects to consider is that the grid-cell values obtained by the spatial interpolation represent areal mean estimates of temperature and precipitation. The punctual conditions at single station sites, especially the daily precipitation peaks, result to be smoothed after the spatialization so that the fine resolution of the daily grids does not correspond to the

250   scales effectively resolved, which are limited by the horizontal spacing of the station network.

The accuracy of the gridded dataset of daily mean temperature and precipitation was evaluated by applying the anomaly-based reconstruction scheme to simulate the daily records of all stations in Trentino – South Tyrol over the study period 1980 – 2018 in a leave-one-out approach, i.e. by removing the station data under evaluation in order to avoid self-influence. The same approach was also applied to assess the errors of the interpolated 1981 – 2010 monthly climatologies, separately. The

255   reconstruction accuracy was computed by comparing the simulations and observations in terms of mean error (BIAS), mean absolute error (MAE), root mean square error (RMSE) and correlation. For daily temperature reconstruction, the resulting BIAS, as average over all stations and whole time period, was almost zero and a MAE (RMSE) of around 1.5 °C (1.9 °C) was obtained. The agreement between daily observations and simulations was high with a mean Pearson correlation coefficient of 0.97 (Fig. 5a). As regards the extremes, the correlation was still high if only the temperature values above 95th percentiles were

260   considered with a mean Pearson coefficient of 0.94 (Fig. 5b), while a slight overestimation was observed for the simulation of temperature records below the 5th percentile (Fig. 5c). The reconstruction errors and correlation by months were also evaluated (Table 1). MAE ranges from 1.1 °C in July to 1.8 °C in October, when the lowest correlation (0.80) was also obtained. BIAS is within -0.5 – 0.5 °C in all months. The simulated 1981 – 2010 monthly mean temperature climatologies at all station sites in the study region showed zero BIAS and MAE (RMSE) ranging from 0.5 (0.6) °C in May to 0.9 (1.1) °C in January (Table

265   2).
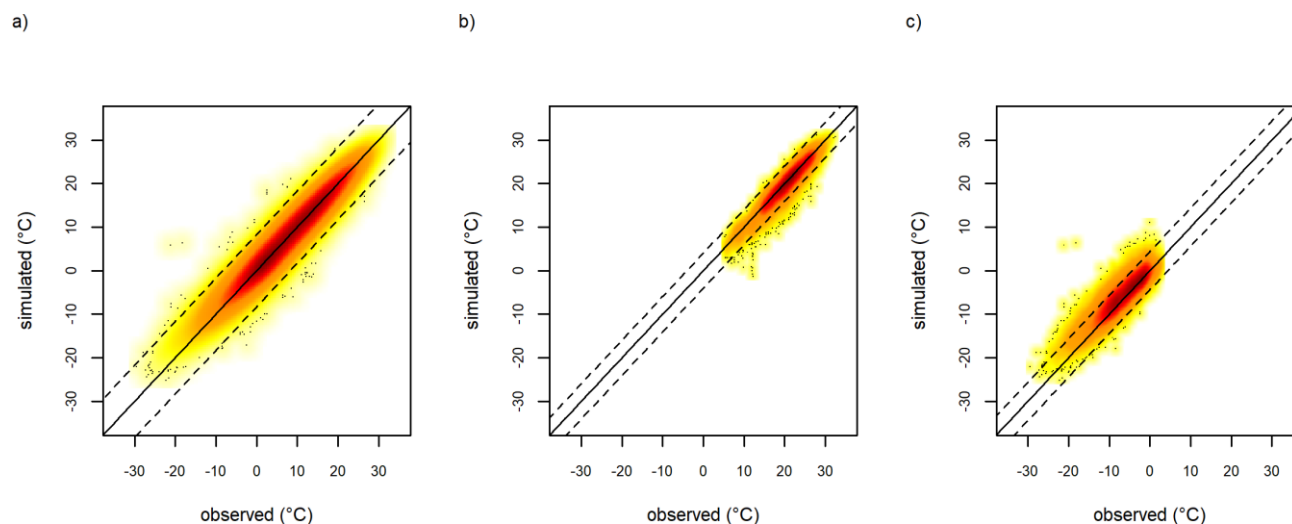
Figure 5: Comparison between simulated and observed daily mean temperature values over the period 1980 – 2018 by considering a) all records, b) the values greater than the 95th percentile and c) the values below the 5th percentile. The dotted straight lines represent ± 1 standard deviation of the data.

MONTH	Daily mean temperature				Daily precipitation			
	BIAS (°C)	MAE (°C)	RMSE (°C)	CORR	BIAS (mm)	MAE (mm)	RMSE (mm)	CORR
1	0.1	1.5	1.9	0.88	0.0	0.6	2.0	0.91
2	-0.2	1.5	1.9	0.90	0.0	0.6	2.1	0.91
3	0.5	1.5	1.9	0.89	0.0	0.7	2.3	0.90
4	-0.1	1.5	1.8	0.86	0.0	1.0	2.6	0.92
5	0.4	1.5	1.9	0.85	0.0	1.4	3.2	0.91
6	0.1	1.3	1.6	0.90	0.0	1.6	3.6	0.88
7	0.3	1.1	1.4	0.91	0.0	1.7	4.1	0.86
8	0.3	1.1	1.4	0.90	0.0	1.6	3.9	0.87
9	-0.4	1.5	1.9	0.82	0.0	1.1	3.3	0.92
10	0.4	1.8	2.2	0.80	0.0	1.1	3.5	0.94
11	-0.2	1.7	2.1	0.84	0.0	1.1	3.3	0.94
12	-0.3	1.6	2.0	0.87	0.0	0.7	2.4	0.92

Table 1: Monthly mean leave-one-out reconstruction errors and correlation for Trentino – South Tyrol daily mean temperature and daily precipitation series over the period 1980 – 2018. BIAS is computed as difference between simulations and observations.

For precipitation, the reconstruction errors by averaging over all stations and daily records showed a MAE (RMSE) of 1.1 (3.2) mm, zero BIAS and a mean correlation coefficient of 0.91. By considering wet days only, i.e. daily precipitation values ≥ 1 mm, the mean correlation decreased to 0.87 and errors increased with mean BIAS of -0.6 mm and MAE (RMSE) of 3.4 (5.8) mm, suggesting a tendency to underestimate the higher precipitation records. The mean monthly errors ranged from 0.6 in January to 1.7 mm in July for MAE and from 2.0 mm in January to 4.1 mm in July for RMSE (Table 1). As regards the precipitation climatological reconstruction, BIAS is below 0.5 mm in all months and MAE (RMSE) ranges from 4.1 (5.6) mm

in February to 10.7 (14.2) mm in November (Table 2). An important source of uncertainty affecting precipitation records, especially in mountain environment, is the well-known "rain-gauge undercatch" which could be particularly relevant during episodes of strong wind and solid precipitation and could account up to several tens of percent of the measured values (Frei

275   and Schär, 1998: Sevruk et al., 2009). Several approaches were developed to account for the undercatch at station sites (see e.g. Grossi et al., 2017), however the magnitude of correction is highly variable with locations, instrumental types and seasons and unproper corrections could reduce the general accuracy of the dataset. For this reason, the contribution of rain-gauge undercatch was neglected in the current analyses.

MONTH	monthly mean temperature climatologies				monthly precipitation climatologies		
	BIAS (°C)	MAE (°C)	RMSE (°C)		BIAS (mm)	MAE (mm)	RMSE (mm)
1	0.0	0.9	1.1		0.1	5.2	7.1
2	0.0	0.7	0.9		0.2	4.1	5.6
3	0.0	0.6	0.7		0.3	5.5	7.5
4	0.0	0.5	0.6		0.2	8.2	11.8
5	0.0	0.5	0.6		-0.1	8.4	11.5
6	0.0	0.5	0.7		-0.1	7.9	10.3
7	0.0	0.5	0.7		0.1	7.4	9.6
8	0.0	0.5	0.7		0.3	7.1	9.3
9	0.0	0.5	0.7		0.1	7.4	9.6
10	0.0	0.6	0.7		0.2	9.2	12.3
11	0.0	0.7	0.8		0.3	10.7	14.2
12	0.0	0.8	1.0		0.1	7.2	10.1

Table 2: Monthly mean leave-one-out reconstruction errors of the 1981 – 2010 monthly mean temperature and precipitation climatologies for Trentino – South Tyrol sites. BIAS is computed as difference between simulations and observations.

Due to the high variability of interpolation errors with the daily precipitation intensity, the comparison between simulated and

280   observed precipitation in wet days during winter and summer was assessed by splitting the data for intensity intervals (Fig. 6). Figure 6 confirms the general tendency of the daily reconstruction method to underestimate intense daily precipitation totals, especially in summer when the underestimation in simulations for the highest quantile interval (0.98 – 0.999) is in median about 24%. On the contrary, overestimation of the lowest quantiles (0.1 – 0.2) in summer was depicted with a median exceedance of 30%. The greater difficulty in simulating summer precipitation could be mostly ascribed to the higher spatial

285   variability of summer precipitation events, mainly driven by convection.

In order to assess also the temporal variability of the dataset uncertainty over the study period and the influence of changes in data coverage over time, the daily simulations and observations were aggregated at monthly scale and reconstruction errors were evaluated for each month over all available stations. The annual averages of monthly errors over 1980 – 2018 are reported in Fig. 7. It is worth noting that the values are almost stable over the whole period for both temperature and precipitation with

290   MAE around 0.7 °C and 13 mm, respectively. However, temperature errors slightly decreased after 1990, as a consequence of

the increase in station density (see Fig. 4a). As regards precipitation, a greater error variability can be observed after 2000 probably due to the changes occurred in station networks during the transition from the manual to automatic rain gauges.

a)

b)
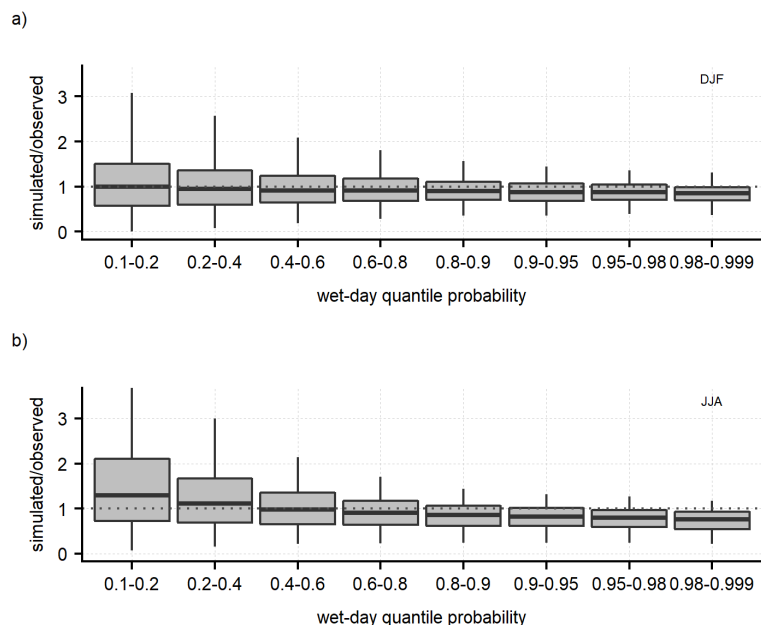
Figure 6: Ratio between daily simulated and observed precipitation (wet days only) in a) winter and b) summer over 1980 – 2010 grouped for quantiles. Boxplots extend over the interquartile range with the median reported by the bold line, while whiskers extend over the full range of outliers.
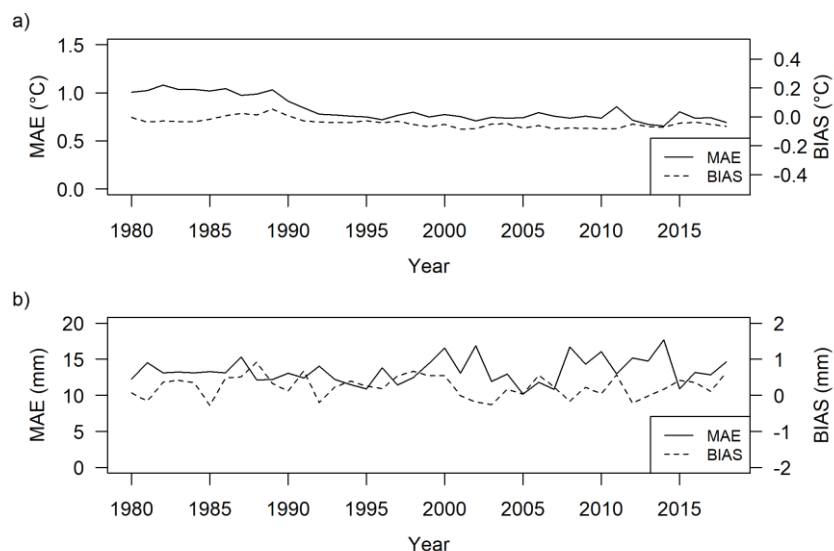
Figure 7: Annual series of mean monthly leave-one-out reconstruction errors (MAE and BIAS) of a) temperature and b) precipitation over the study period for the available stations in Trentino – South Tyrol.

3.2 The gridded dataset: regional climatic features, example cases and snow-cover comparison

The 250 m gridded dataset allows to discuss and analyse the main features of the climate in the region. In the following, the

295 30 year annual climatologies of mean temperature and total precipitation over the period 1981 – 2010 are shown in Fig. 8. The derived features were largely in agreement with the findings of previous works focusing on the regional climate (e.g. Adler et al., 2015), and the 250 m grid spacing allows a detailed visualization of the spatial patterns. The mean annual temperature ranges from +14 °C in the Garda Valley located in the southernmost part of the region to about -11 °C at the Ortles peak with an average value of around +5 °C over the entire study region. The thermal contrast between the inner valleys and the steep

300 surrounding reliefs is well depicted. Mean annual values are around +12 °C in the main valley bottoms, while the isothermal of 0 °C occurs at about 2400 m. The annual cycle of mean temperature, as average over the region and based on the 1981 – 2010 normals, is characterized by the warmest conditions in July while the coldest month is January with -3.2 °C (Fig. 9). The greatest warming occurs between April and May, when also the thermal range between the coldest and the hottest locations increases reaching the maximum between May and June with almost 30 °C. The most relevant cooling is depicted in the

305 transition from October to November when the isothermal of 0 °C drops from around 2700 to 1700 m and the occurrence of cold air pools in the valleys becomes more frequent.
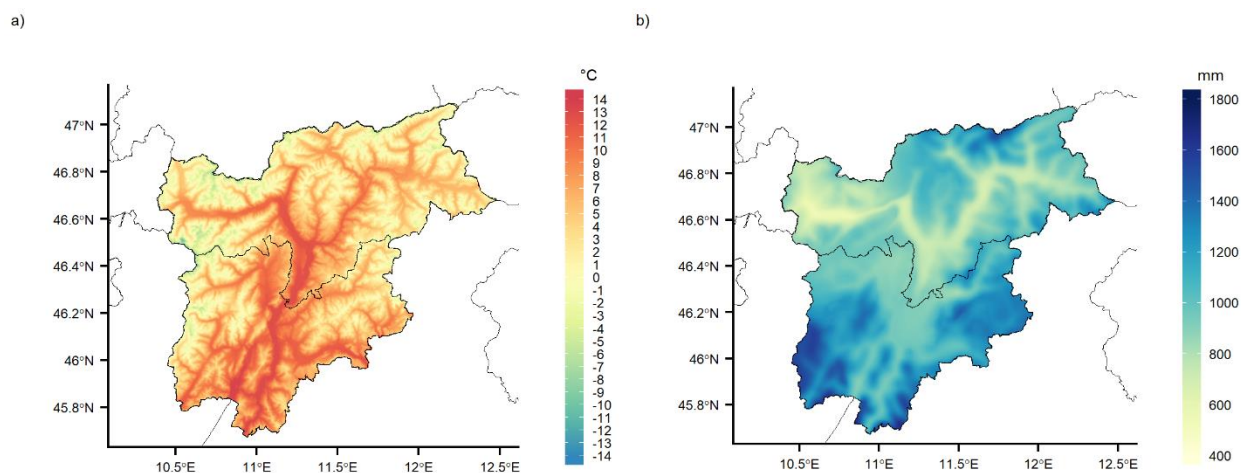
Figure 8: 1981 – 2010 annual a) mean temperature and b) total precipitation climatologies (250 m grid spacing) over Trentino – South Tyrol.

Topographic effects are also evident in the precipitation distribution over the study region. Annual totals range from 530 mm in the inner Venosta Valley (north-western South Tyrol) to more than 1700 mm in the southernmost part of the region, where wet southerly flows are more relevant. The mean annual precipitation sum is around 1000 mm as spatial average over the

310 whole region, with drier conditions in the northern inner valleys of South Tyrol with annual totals around 900 mm. As regards the mean annual cycle, the driest conditions occur in late winter, with a minimum in February when the mean regional totals are below 40 mm. On the contrary, precipitation significantly increases in May, with the growing contribution of local convection, and the annual maximum is reached in July, with a regional average of almost 120 mm. Regional mean

precipitation values show a secondary minimum in September and increase again in October, when greater contrasts over the
315 region, especially between north and south, are depicted with the wettest contributions in the Trentino valleys, more exposed
to humid air masses coming from the Mediterranean sea .

By focusing on distinct portions of the study area, a relevant sub-regional variability can be observed (Fig. 10). In particular,
a different annual precipitation cycle characterizes the northern and southern portions of the study region. In the northern and
central parts the precipitation cycle has a maximum in summer and the peak increases moving from west (Venosta Valley),
320 where rain-shadow effects are more frequent, to east, where the Alpine ridge receives wet contributions from both northerly
and southerly flows. On the contrary, the annual cycle in the south of the region shows two precipitation maxima occurring in
spring and autumn. The influence of subtropical high-pressure areas is particularly relevant for the southernmost valleys and
contributes to the drying tendencies over summer months which defines here the local precipitation minimum.
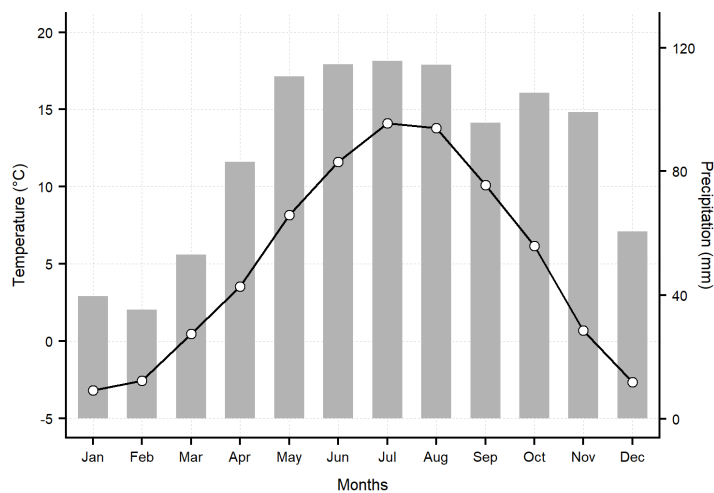
Figure 9: Mean regional annual cycle of monthly mean temperature and total precipitation based on the 1981 – 2010 climatologies.
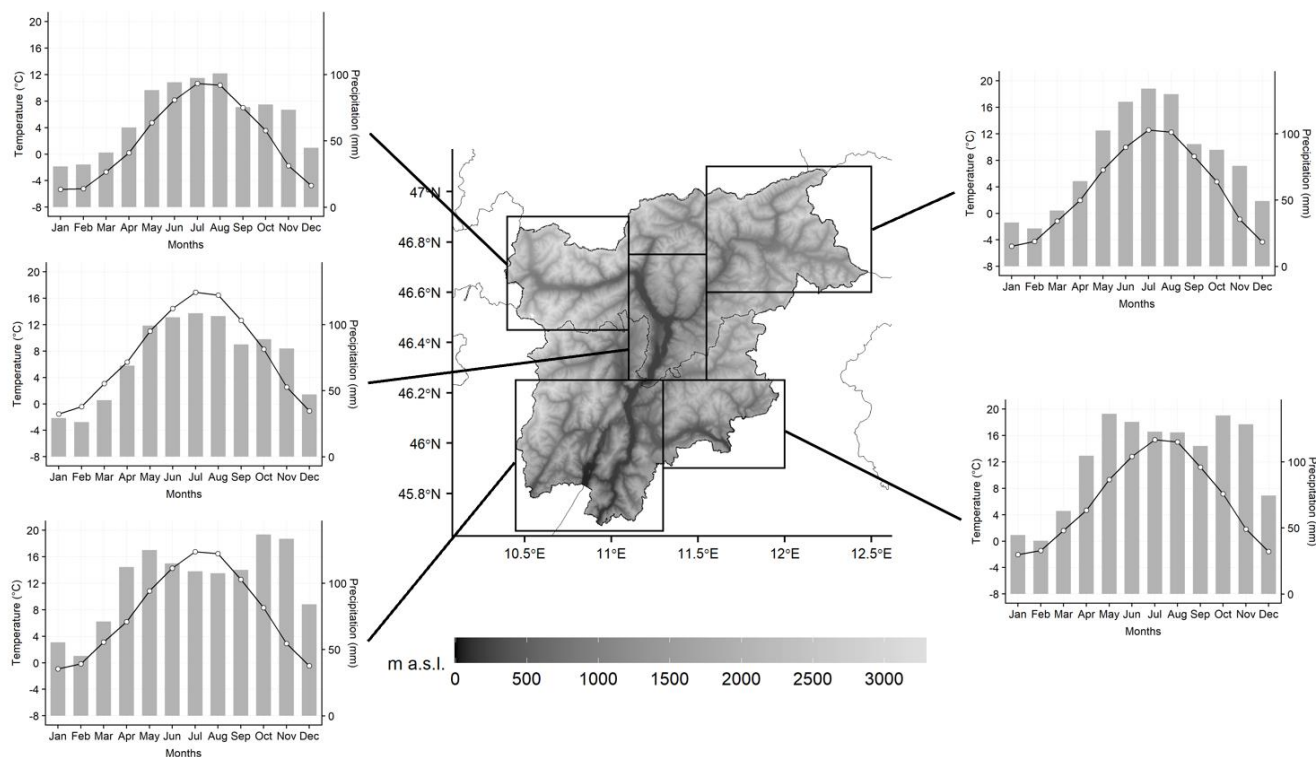
Figure 10: Mean sub-regional annual cycles of monthly mean temperature and total precipitation based on the 1981 – 2010 climatologies for five distinct areas.

Among the useful applications of high-resolution gridded climate variables at daily timescale, they allow to study and

325   reconstruct past episodes of particular interest, such as intense precipitation events, and their temporal day-by-day pattern over the entire region. In particular, we reported as example cases the computed 250 m daily fields for two past episodes experiencing meteorological extremes over the region.

One of the most recent intense events occurred on 27–30 October 2018 when an intense storm affected a large portion of eastern Italian Alps leading to severe impacts, such as floods, landslides, interruption of traffic and electricity supply and

330   severe forest damages due to intense wind gusts up to 200 km h^{-1} (Dalponte et al., 2020; Davolio et al., 2020). During this event, exceptional amounts of precipitation were recorded in few days at many locations. In Fig. 11, the 4 day precipitation sum over 27–30 October 2018 is reported together with the daily anomalies with respect to the 1981 – 2010 monthly normals for the month. In some areas, especially the upper Isarco Valley in the northern of South Tyrol, the south western portion of Trentino and along its eastern border with Veneto region, precipitation amounts were particularly intense, with 4 day totals

335   locally exceeding 500 mm (Fig. 11a). Over the whole region, the 4 day precipitation totals were greater than the monthly normals for October, with 80% of the grid points with precipitation amounts more than double the climatological totals for the month (Fig. 11b). As discussed in Sect. 3.1, the reported daily fields provide a comprehensive overview of the precipitation patterns over the region and the locations of the maxima, however the applied daily interpolation based on weighted spatial

average has a smoothing effect so that the daily gridded fields are expected to underestimate the very localized peaks at
340 individual stations.
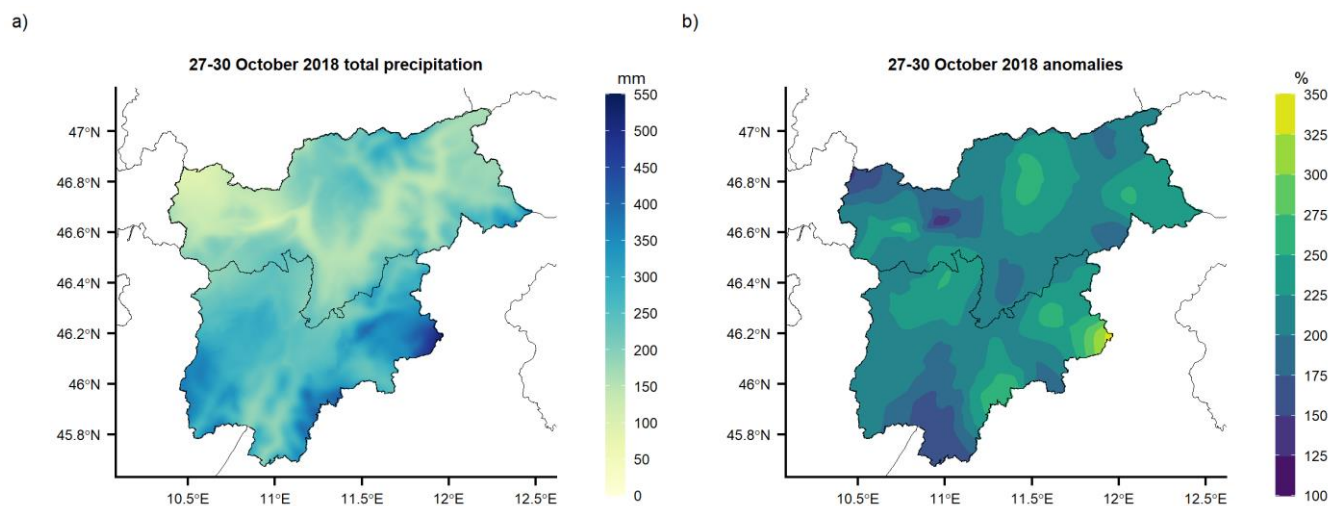
Figure 11: Event of October 2018 over Trentino – South Tyrol: a) 4 day total precipitation over 27–30 October 2018 (250 m spatial resolution) and b) relative anomalies of the 4 day totals with respect to the 1981 – 2010 monthly normals of total precipitation for October.

As second example case, the summer 2003 was considered when exceptionally high temperature values were recorded in a large part of western Europe due to the influence of sub-tropical air masses and the presence of a wide high-pressure system over Europe. The high temperatures and the relatively scarce precipitation occurred in the previous winter and spring months fostered drought conditions in several regions. In Trentino – South Tyrol the mean temperature anomalies over the summer
345 period were, as average over the region, around +3 °C with respect to the reference 1981 - 2010 normals (Fig 12a). In particular, August was the hottest month and the greatest temperature values were reached on 11 August with a mean temperature on regional level greater than 21 °C and daily maximum temperature close to +40 °C in Bolzano and Trento. The distribution of the daily mean temperature on 11 August shows values above +30 °C along the main valley bottoms (Fig. 12b) and over almost the whole region the daily values exceed the climatological means with a mean anomaly of about +7 °C for that day.
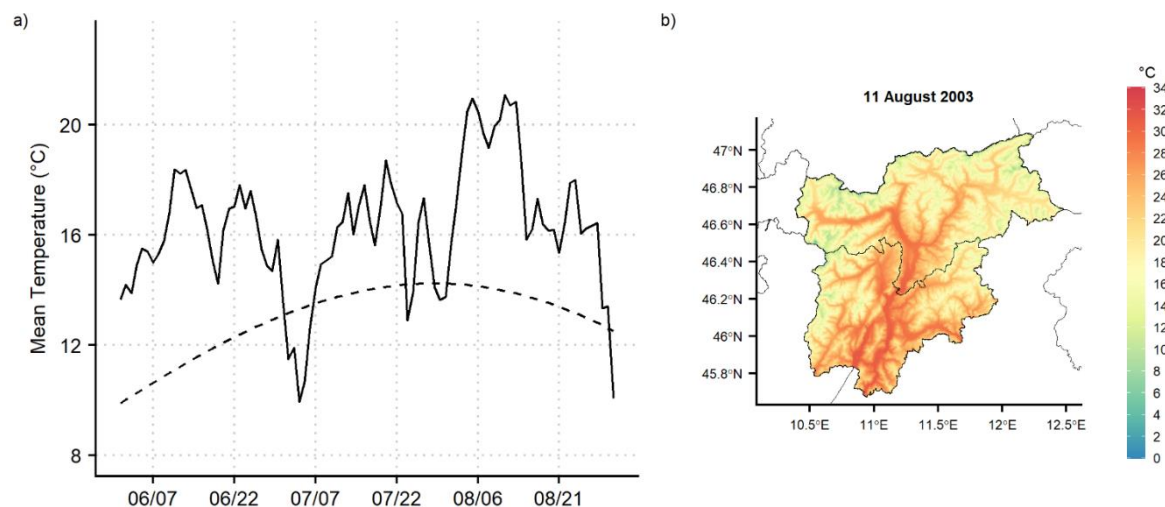
Figure 12: in panel a) the regional daily mean temperature series for summer 2003 is shown (solid line) together with the 1981 – 2010 daily normals (dashed line); in panel b) the spatial distribution over Trentino – South Tyrol of mean temperature on the hottest summer day in 2003 (11 August) is reported at 250 m grid spacing.

In order to evaluate the suitability of the gridded meteorological data to be integrated with other high-resolution products, the dataset of mean temperature and precipitation was compared to a 250 m resolution daily dataset of snow cover over the region. The daily snow-cover maps used for the comparison are based on Moderate Resolution Imaging Spectroradiometer (MODIS) images and provide binary snow-cover information (snow, snow free) using an algorithm tailored to complex terrain (Notarnicola et al., 2013). In this product, clouds were interpolated in Terra-only images yielding almost cloud-free daily maps for the period 2000 – 2018 (Matiu et al., 2020a). Starting from the snow-cover data, the snow-cover duration (SCD) over the winter season (December, January and February) was computed at each grid point of the study domain and the Pearson correlation with the mean winter temperature and total winter precipitation was computed over all available winters of SCD data (2001 – 2018). Since SCD saturates at high elevations preventing from computing the correlation coefficients, all points above 2500 m were excluded from the analysis. As expected, correlation coefficients with temperature are negative within the inter-quantile range (25th – 75th percentiles) for all elevation intervals (Table 3). The anticorrelation decreases with increasing elevation with median values ranging from -0.55 below 500 m to -0.41 above 1500 m. On the contrary, the correlation with total winter precipitation is positive within the inter-quantile range in all cases and a clear elevation dependency is evident with correlation values increasing with altitudes, up to 0.55 as median in the range 1500–1750 m. In considering the behaviour of SCD correlation with temperature and precipitation over different elevation bands, the effect of winter SCD saturation with increasing elevation should be taken into account. This could partly explain the increase of the anticorrelation with temperature and the concurrent decrease of precipitation–SCD dependency in the upper elevation bands (above 1750 m). These outcomes are in agreement with other literature studies investigating the dependency of several snow parameters with temperature and elevation in the Alps (see e.g. Móran-Tejeda et al., 2014; Schöner et al., 2019; Matiu et al., 2020b) and specifically in Trentino region (Marcolini et al., 2017).

Elevation interval (m)	SCD and T_m correlation			SCD and P correlation		
	25th percentile	Median	75th percentile	25th percentile	Median	75th percentile
< 500	-0.63	-0.55	-0.44	0.01	0.14	0.28
500 - 750	-0.60	-0.51	-0.38	0.14	0.28	0.43
750 - 1000	-0.60	-0.49	-0.33	0.25	0.39	0.52
1000 - 1250	-0.58	-0.45	-0.27	0.34	0.47	0.58
1250 - 1500	-0.56	-0.42	-0.25	0.40	0.52	0.64
1500 - 1750	-0.52	-0.41	-0.26	0.43	0.55	0.66
1750 - 2000	-0.51	-0.43	-0.34	0.34	0.43	0.56
2000 - 2500	-0.50	-0.44	-0.37	0.10	0.25	0.36

Table 3: Median and inter-quantile range of 2001 – 2018 correlation coefficients over different elevation bands between SCD (snow-cover duration) and a) mean temperature and b) total precipitation in winter season (December, January and February). Only grid points below 2500 m are considered.
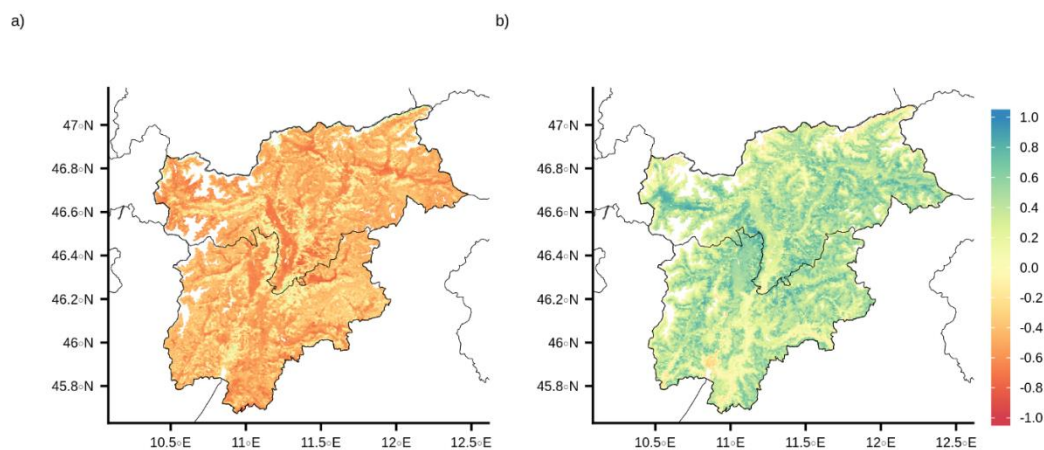
Figure 13: Spatial distribution of 2001 – 2018 correlation coefficients over the region between SCD (snow-cover duration) and a) mean temperature and b) total precipitation in winter season (December, January and February). White areas correspond to masked grid points (above 2500 m) or to missing snow cover data.

The elevation dependency of winter SCD correlation with temperature and precipitation is also highlighted in the spatial distribution of the coefficients over the region (Fig. 13). The greatest anticorrelation with temperature is depicted along the

375 main valley floors, especially Adige and Isarco Valleys, while the greatest dependency with precipitation is pointed out along the mid-elevation zones decreasing towards both lower elevations, where winter precipitation occurs generally in liquid form, and higher altitudes where snowfalls usually occur in winter season and, regardless of their magnitude, snow lasts on the ground due to the relatively low temperature.

4 Codes and data availability

380 The dataset of daily mean temperature and total precipitation at 250 m resolution spanning the period 1980 – 2018 for Trentino – South Tyrol and the 250 m resolution 1981 – 2010 monthly climatologies are freely available at PANGAEA Data Publisher for Earth and Environmental Science through https://www.pangaea.de/tok/2bea918566a8c18a728e098858856cd1fcc8dbe4, Crespi et al. (2020). The data are stored in NetCDF format that eases the processing in scientific programming software (e.g. Python and R) and GIS. The dataset of daily snow cover used for the comparison is freely available from Matiu et al. (2019).

385 All routines are developed in R environment and are available upon request from the authors.

5 Conclusions

The 250 m resolution dataset of daily mean temperature and total precipitation for Trentino – South Tyrol region over 1980 – 2018 was presented. It was derived starting from a dense database of more than 200 station observations, covering the region and close surroundings, which were all checked for quality and homogeneity. The gridded daily fields were computed by

390 applying an interpolation procedure in which the 30 year climatologies (1981 – 2010) and the daily anomalies were combined. In this procedure, the local relationship between the climate variables and the orography are considered for the climatology spatialization, while the station daily anomalies are interpolated by a weighted-averaging approach. The method was demonstrated to be particularly robust in reconstructing climate fields in mountain areas, where systematic errors, especially precipitation underestimations, could occur due to the uneven data coverage, e.g. between low and high-elevation areas.

395 The leave-one-out cross-validation pointed out the overall robustness of gridded fields for both daily temperature and precipitation with mean correlation coefficients above 0.80 in all months and MAE, as average over all stations and months, of around 1.5 °C for mean temperature and 1.1 mm for precipitation. Moreover, the reconstruction errors showed to be almost constant over the whole study period, despite the changes in available station number, especially during the first decade.

The provided dataset represents a valuable archive of continuous climate information for the region, spanning almost 40 years,

400 and the very fine grid spacing facilitates its application for a wide range of scopes requiring spatially explicit fields of climate variables, such as hydrological analyses, environmental modelling, impact studies and remote sensing data validation. The availability of gridded information allows to derive more accurate aggregations and spatial averages over specific sub-domains, e.g. at catchment and sub-catchment levels, than averaging the single station records directly. Other potential applications include the downscaling of climate change scenarios and the improved evaluations of high-resolution regional climate models.

405 However, it is necessary to take into account for any application that the spatial scales effectively resolved by the dataset at daily resolution are coarser than the nominal grid spacing and in the order of several km, i.e. close to the mean inter-station distance, and systematic errors in punctual values cannot be avoided, such as underestimation of the highest intensities. Possible improvements in spatial representativeness could be derived by the integration of additional in situ observations and/or by evaluating alternative and more sophisticated interpolation techniques for modelling the small-scale interactions

410 between climate variables and orography.

Despite the intrinsic issues, the dataset allows to extract and analyse the fine scale distribution of the main climatic features over the region, which are described by the 1981 – 2010 monthly climatologies. The suitability of the daily fields in representing the spatial structure of specific events of interest was discussed and example cases of intense past episodes were reported. In order to better investigate the potential applications of this fine-scale product, we also performed a preliminary

415   comparison between the gridded meteorological variables and the 250 m MODIS SCD winter maps. The pointwise correlation analysis over the period 2001 – 2018 pointed out a clear elevation dependency of SCD to both temperature and precipitation and the fine spatial scale led to a more detailed insight on the spatial distribution over the region of these relationships suggesting interesting open questions which require to be further developed in forthcoming works.

The dataset is intended to be integrated in the next future by the gridded fields of daily maximum and minimum temperature

420   and to be converted into a near-real time product including regular updates and supporting operational applications at local and regional levels.

Author contributions

AC designed and applied the interpolation scheme. The data collection and processing were performed by AC in collaboration with MM and GB. The validation analyses were carried out by AC, MP contributed in the discussion of the interpolation errors

425   and MM provided snow cover data and helped in the interpretation of the results. MZ supervised and supported all the phases of the work. AC prepared the manuscript with the collaboration of all co-authors.

Competing interests

The authors declare that they have no conflict of interest.

Acknowledgments

430   The authors thank the Hydrographic Office of the Autonomous Province of Bolzano and Meteotrentino for the provision of the meteorological data for the study region and ARPA Veneto, ZAMG, the HISTALP project and MeteoSwiss which provided the series used for the extra regional sites. Prof. Majone and prof. Bellini from the University of Trento are also acknowledged for providing useful information on available data and products. The research leading to these results has received funding from the European Regional Development Fund, Operational Programme Investment for growth and jobs ERDF 2014-2020

435   under Project number ERDF1094, Data Platform and Sensing Technology for Environmental Sensing LAB – DPS4ESLAB.

References

Aadhar, S. and Mishra, V.: High-resolution near real-time drought monitoring in South Asia, Sci Data, 4, 170145, doi:10.1038/sdata.2017.145, 2017.

Adler, S., Chimani, B., Drechsel, S., Haslinger, K., Hiebl, J., Meyer, V., Resch, G., Rudolph, J., Vergeiner, J., Zingerle, C., et
440   al. Das Klima: Von Tirol-Sudtirol-Belluno, ZAMG, Autonome Provinz Bozen, ARPAV, Eds. 2015. Available online: http://www.3pclim.eu/images/Das_Klima_von_Tirol-Suedtirol-Belluno.pdf (accessed on 12 October 2020).

Auer, I., Böhm, R., Jurkovic, A., Lipa, W., Orlik, A., Potzmann, R., Schöner, W., Ungersböck, M., Matulla, C., Briffa, K., Jones, P., Efthymiadis, D., Brunetti, M., Nanni, T., Maugeri, M., Mercalli, L., Mestre, O., Moisselin, J., Begert, M., Müller-Westermeier, G., Kveton, V., Bochnicek, O., Stastny, P., Lapin, M., Szalai, S., Szentimrey, T., Cegnar, T., Dolinar, M., Gajic-
445   Capka, M., Zaninovic, K., Majstorovic, Z., and Nieplova, E.: HISTALP – Historical instrumental climatological surface time series of the Greater Alpine Region HISTALP, Int. J. of Climatol., 27, 17–46, doi:10.1002/joc.1377, 2007.

Beven, K., Cloke, H., Pappenberger, F., Lamb, R., and Hunter, N.: Hyperresolution information and hyperresolution ignorance in modelling the hydrology of the land surface, Science China Earth Sciences, 58, 25—35, doi:10.1007/s11430-014-5003-4, 2015.

450   Brunetti, M., Maugeri, M., Monti, F., and Nanni, T.: Temperature and precipitation variability in Italy in the last two centuries from homogenised instrumental time series, Int. J. of Climatol., 26, 345–381, doi:10.1002/joc.1251, 2006.

Brunetti, M., Lentini, G., Maugeri, M., Nanni, T. and Spinoni, J.: Projecting North Eastern Italy temperature and precipitation secular records onto a high-resolution grid, Phys. Chem. Earth, Parts A/B/C, 40–41, 9–22, doi:10.1016/j.pce.2009.12.005, 2012.

455   Brunetti, M., Maugeri, M., Nanni, T., Simolo, C., and Spinoni, J.: High-resolution temperature climatology for Italy: interpolation method intercomparison, Int. J. Climatol., 34, 1278–1296, doi:10.1002/joc.3764, 2014.

Brunsdon, C., McClatchey, J., and Unwin, D.: Spatial variations in the average rainfall–altitude relationship in Great Britain: an approach using geographically weighted regression, Int. J. Climatol., 21, 455–466, doi:10.1002/joc.614, 2001.

Camera, C., Bruggeman, A., Hadjinicolaou, P., Pashiardis, S., and Lange, M. A.: Evaluation of interpolation techniques for
460   the creation of gridded daily precipitation (1×1 km^2); Cyprus, 1980–2010, J. Geophys. Res. Atmos., 119, 693–712, doi:10.1002/2013JD020611, 2014.

Chimani, B., Matulla, C., Böhm, R., and Hofstätter, M.: A new high resolution absolute temperature grid for the Greater Alpine Region back to 1780, Int. J. Climatol., 33, 2129–2141, doi:10.1002/joc.3574, 2013.

Craddock, J.: Methods of comparing annual rainfall records for climatic purposes, Weather, 34, 332–346, doi:10.1002/j.1477-
465   8696.1979.tb03465.x, 1979.

Crespi, A., Brunetti, M., Lentini, G., and Maugeri, M.: 1961-1990 high-resolution monthly precipitation climatologies for Italy, Int. J. Climatol., 3, 878–895, doi:10.1002/joc.5217, 2018.

Crespi, A., Matiu, M., Bertoldi, G., Petitta, M., and Zebisch, M.: High-resolution daily series (1980 - 2018) and monthly climatologies (1981 - 2010) of mean temperature and precipitation for Trentino - South Tyrol (north-eastern Italian Alps).

470   PANGAEA, https://doi.pangaea.de/10.1594/PANGAEA.924502, 2020 (in review).

Crespi, A., Brunetti, M., Ranzi, R., Tomirotti, M., and Maugeri, M.: A multi-century meteo-hydrological analysis for the Adda river basin (Central Alps). Part I: Gridded monthly precipitation (1800–2016) records, Int. J. Climatol., 41, 162–180, doi:10.1002/joc.6614, 2021.

Dalponte, M., Marzini, S., Solano-Correa, Y. T., Tonon, G., Vescovo, L., and Gianelle, D.: Mapping forest windthrows using

475   high spatial resolution multispectral satellite images, Int. J. Appl. Earth Obs. Geoinf., 93, 102206, doi:10.1016/j.jag.2020.102206, 2020.

Daly, C., Gibson, W. P., Taylor, G. H., Johnson, G. L., and Pasteris, P.: A knowledge-based approach to the statistical mapping of climate, Clim. Res., 22, 99–113, doi:10.3354/cr022099, 2002.

Daly, C., Smith, J. W., Smith, J. I., and McKane, R. B.: High-Resolution Spatial Modeling of Daily Weather Elements for a

480   Catchment in the Oregon Cascade Mountains, United States, J. Appl. Meteor. Climatol., 46, 1565–1586, doi:10.1175/JAM2548.1, 2007.

Davolio, S., Della Fera, S., Laviola, S., Miglietta, M. M., and Levizzani, V.: Heavy Precipitation over Italy from the Mediterranean Storm "Vaia" in October 2018: Assessing the Role of an Atmospheric River. Mon. Wea. Rev., 148, 3571–3588, doi:10.1175/MWR-D-20-0021.1, 2020.

485   Di Piazza, A., Conti, F. L., Noto, L., Viola, F., and La Loggia, G.: Comparative analysis of different techniques for spatial interpolation of rainfall data to create a serially complete monthly time series of precipitation for Sicily, Italy, Int. J. Appl. Earth Obs. Geoinform., 13, 396–408, doi:10.1016/j.jag.2011.01.005, 2011.

Durre, I., Menne, M. J., Gleason, B. E., Houston, T. G., and Vose, R. S.: Comprehensive Automated Quality Assurance of Daily Surface Observations, J. Appl. Meteor. Climatol., 49, 1615–1633, doi:10.1175/2010JAMC2375.1, 2010.

490   Engelhardt, M., Schuler, T. V., and Andreassen, L. M.: Contribution of snow and glacier melt to discharge for highly glacierised catchments in Norway, Hydrol. Earth Syst. Sci., 18, 511–523, doi:10.5194/hess-18-511-2014, 2014.

Fick, S. E. and Hijmans, R. J.: WorldClim 2: new 1-km spatial resolution climate surfaces for global land areas, Int. J. Climatol., 37, 4302–4315, doi:10.1002/joc.5086, 2017.

Foresti, L., Sideris, I., Panziera, L., Nerini, D., and Germann, U.: A 10-year radar-based analysis of orographic precipitation

495   growth and decay patterns over the Swiss Alpine region, Q. J. Roy. Meteor. Soc., 144, 2277–2301, doi:10.1002/qj.3364, 2018.

Frei, C. and Schär, C.: A precipitation climatology of the Alps from high-resolution rain-gauge observations, Int. J. Climatol., 18, 873–900, doi:10.1002/(SICI)1097-0088(19980630)18:8<873::AID-JOC255>3.0.CO;2-9, 1998.

Grasso, L. D.: The differentiation between grid spacing and resolution and their application to numerical modeling, B. Am. Meteorol. Soc., 81, 579–580, doi:10.1175/1520-0477(2000)081<0579:CAA>2.3.CO;2, 2000.

500   Grossi, G., Lendvai, A., Peretti, G., and Ranzi, R.: Snow Precipitation Measured by Gauges: Systematic Error Estimation and Data Series Correction in the Central Italian Alps, Water, 9, 461, doi:10.3390/w9070461, 2017.

Harris, I., Jones, P., Osborn, T., and Lister, D.: Updated high-resolution grids of monthly climatic observations – the CRU TS3.10 Dataset, Int. J. Climatol., 34, 623–642, doi:10.1002/joc.3711, 2014.

Haylock, M. R., Hofstra, N., Klein Tank, A. M. G., Klok, E. J., Jones, P. D., and New, M.: A European daily high-resolution
505   gridded data set of surface temperature and precipitation for 1950–2006, J. Geophys. Res., 113, D20119, doi:10.1029/2008JD010201, 2008.

Hengl, T.: A Practical Guide to Geostatistical Mapping, ISBN 978–90–9024981-0. Licensed under a creative Commons Attribution-Noncommercial-No Derivative Works 3.0 license. Available at http://spatial-analyst.net/book/, 2009.

Hiebl, J. and Frei, C.: Daily precipitation grids for Austria since 1961—development and evaluation of a spatial dataset for
510   hydroclimatic monitoring and modelling, Theor. Appl. Climatol., 132, 327–345, doi:10.1007/s00704-017-2093-x, 2018.

Hofstra, N., Haylock, M., New, M., Jones, P., and Frei, C.: Comparison of six methods for the interpolation of daily European climate data, J. Geophys. Res., 113, D21110, doi:10.1029/2008JD010100, 2008.

Hofstra, N., New, M., and McSweeney, C.: The influence of interpolation and station network density on the distributions and trends of climate variables in gridded daily data, Clim. Dyn., 35, 841–858. doi:10.1007/s00382-009-0698-1, 2010.

515   Immerzeel, W. W., Lutz, A. F., Andrade, M., Bahl, A., Biemans, H., Bolch, T., Hyde, S., Brumby, S., Davies, B. J., Elmore, A. C., Emmer, A., Feng, M., Fernández, A., Haritashya, U., Kargel, J. S., Koppes, M., Kraaijenbrink, P. D. A., Kulkarni, A. V., Mayewski, P. A., Nepal, S., Pacheco, P., Painter, T. H., Pellicciotti, F., Rajaram, H., Rupper, S., Sinisalo, A., Shrestha, A. B., Viviroli, D., Wada, Y., Xiao, C., Yao, T., and Baillie J. E. M.: Importance and vulnerability of the world's water towers, Nature, 577, 364–369, doi:10.1038/s41586-019-1822-y, 2020.

520   Isotta, F. A., Frei, C., Weilguni, V., Perčec Tadić, M., Lassègues, P., Rudolf, B., Pavan, V., Cacciamani, C., Antolini, G., Ratto, S. M., Munari, M., Micheletti, S., Bonati, V., Lussana, C., Ronchi, C., Panettieri, E., Marigo, G., and Vertačnik, G.: The climate of daily precipitation in the Alps: development and analysis of a high-resolution grid dataset from pan-Alpine rain-gauge data, Int. J. Climatol., 34, 1657–1675, doi:10.1002/joc.3794, 2014.

Isotta, F. A., Begert, M., and Frei, C.: Long-term consistent monthly temperature and precipitation grid data sets for
525   Switzerland over the past 150 years, J. Geophys. Res.: Atmospheres, 124, 3783–3799, doi:10.1029/2018JD029910, 2019.

Kotlarski, S., Szabó, P., Herrera, S., Räty, O., Keuler, K., Soares, P. M., Cardoso, R. M., Bosshard, T., Pagé, C., Boberg, F., Gutiérrez, J. M., Isotta, F. A., Jaczewski, A., Kreienkamp, F., Liniger, M. A., Lussana, C., and Pianko-Kluczyńska, C.: Observational uncertainty and regional climate model evaluation: A pan-European perspective, Int J Climatol., 39, 3730–3749, doi:10.1002/joc.5249, 2019.

530   Laiti, L., Mallucci, S., Piccolroaz, S., Bellin, A., Zardi, D., Fiori, A., Nikulin, G., and Majone., B.: Testing the hydrological coherence of high-resolution gridded precipitation and temperature data sets, Water Resour. Res., 54, 1999–2016, doi:10.1002/2017WR021633, 2018.

Ledesma, J. L. J. and Futter, M. N.: Gridded climate data products are an alternative to instrumental measurements as inputs to rainfall–runoff models, Hydrol. Process., 31, 3283–3293, doi:10.1002/hyp.11269, 2017.

535 Longman, R. J., Frazier, A. G., Newman, A. J., Giambelluca, T. W., Schanzenbach, D., Kagawa-Viviani, A., Needham, H., Arnold, J. R., and Clark, M. P.: High-Resolution Gridded Daily Rainfall and Temperature for the Hawaiian Islands (1990–2014), J. Hydrometeor., 20, 489–508, doi:10.1175/JHM-D-18-0112.1, 2019.

Lussana, C., Tveito, O. E., Dobler, A., and Tunheim, K.: seNorge_2018, daily precipitation, and temperature datasets over Norway, Earth Syst. Sci. Data, 11, 1531–1551, doi:10.5194/essd-11-1531-2019, 2019.

540 Ly, S., Charles, C., and Degré, A.: Geostatistical interpolation of daily rainfall at catchment scale: the use of several variogram models in the Ourthe and Ambleve catchments, Belgium, Hydrol. Earth Syst. Sci., 15, 2259–2274, doi:10.5194/hess-15-2259-2011, 2011.

Marcolini, G., Bellin, A., Disse, M., and Chiogna, G.: Variability in snow depth time series in the Adige catchment, Journal of Hydrology: Regional Studies, 13, 240–254, doi:10.1016/j.ejrh.2017.08.007, 2017.

545 Matiu, M., Jacob, A., and Notarnicola, C.: Daily MODIS snow cover maps for the European Alps from 2002 onwards at 250m horizontal resolution along with a nearly cloud-free version (Version v1.0.2) [Data set], Zenodo, doi:10.5281/zenodo.3601891, 2019.

Matiu, M., Jacob, A., and Notarnicola, C.: Daily MODIS Snow Cover Maps for the European Alps from 2002 onwards at 250 m Horizontal Resolution Along with a Nearly Cloud-Free Version, Data, 5, 1, doi:10.3390/data5010001, 2020a.

550 Matiu, M., Crespi, A., Bertoldi, G., Carmagnola, C., Marty, C., Morin, S., Schöner, W., Berro, D., Chiogna, G., Gregorio, L., Kotlarski, S., Majone, B., Resch, G., Terzago, S., Valt, M., Beozzo, W., Cianfarra, P., Gouttevin, I., Marcolini, G., Notarnicola, C., Petitta, M., Scherrer, S., Strasser, U., Winkler, M., Zebisch, M., Cicogna, A., Cremonini, R., Debernardi, A., Faletto, M., Gaddo, M., Giovannini, L., Mercalli, L., Soubeyroux, J., Sušnik, A., Trenti, A., Urbani, S., and Weilguni, V.: Observed snow depth trends in the European Alps 1971 to 2019, The Cryosphere Discuss. [preprint], doi:10.5194/tc-2020-289, in review,
555 2020b.

Morán-Tejeda, E., López-Moreno, J. I., and Beniston, M.: The changing roles of temperature and precipitation on snowpack variability in Switzerland as a function of altitude, Geophys. Res. Lett., 40, 2131–2136, doi:10.1002/grl.50463, 2013.

Navarro-Racines, C., Tarapues, J., Thornton, P., Jarvis, H., and Ramirez-Villega, J.; High-resolution and bias-corrected CMIP5 projections for climate change impact assessments, Sci. Data, 7, 7, doi:10.1038/s41597-019-0343-8, 2020.

560 New, M., Todd, M., Hulme, M., and Jones, P.: Precipitation measurements and trends in the twentieth century, Int. J. Climatol., 21, 1899–1922, doi:10.1002/joc.680, 2001.

Notarnicola, C., Duguay, M., Moelg, N., Schellenberger, T., Tetzlaff, A., Monsorno, R., Costa, A., Steurer, C., and Zebisch, M.: Snow Cover Maps from MODIS Images at 250 m Resolution, Part 2: Validation, Remote Sens., 5, 1568–1587, doi:10.3390/rs5041568, 2013.

565 Price, F. M.: Alpenatlas – Atlas des Alpes – Atlante delle Alpi – Atlas Alp – Mapping the Alps: Society – Economy – Environment, edited by Ulrike Tappeiner, Axel Borsdorf, Erich Tasser. Heidelberg, Germany: Spektrum. 2008. ISBN: 978-3-8274-2004-6. Mountain Research and Development: 29. 292–293, doi:10.1659/mrd.mm057, 2009.

Schlögel, R., Kofler, C., Gariano, S. L., Van Campenhout, J., and Plummer, S.: Changes in climate patterns and their association to natural hazard distribution in South Tyrol (Eastern Italian Alps), Sci. Rep., 10, 5022, doi:10.1038/s41598-020-61615-w, 2020.

Schöner, W., Koch, R., Matulla, C., Marty, C., and Tilg, A-M.: Spatiotemporal patterns of snow depth within the Swiss-Austrian Alps for the past half century (1961 to 2012) and linkages to climate change, Int. J. Climatol., 39, 1589–1603, doi:10.1002/joc.5902, 2019.

Sekulić, A., Kilibarda, M., Protić, D., Perčec Tadić, M., and Bajat, B.: Spatio-temporal regression kriging model of mean daily temperature for Croatia, Theor. Appl. Climatol., 140, 101–114, doi:10.1007/s00704-019-03077-3, 2020.

Sevruk, B., Ondrás, M., and Chvíla, B.: The WMO precipitation measurement intercomparisons, Atm. Res., 92, 376–380, doi:10.1016/j.atmosres.2009.01.016, 2009.

Stewart, S. B. and Nitschke, C. R.: Improving temperature interpolation using MODIS LST and local topography: a comparison of methods in south east Australia, Int. J. Climatol., 37(7), 3098–3110, doi:10.1002/joc.4902, 2017.